Transfer of Lipophilic Markers from PLGA and Polystyrene Nanoparticles to Caco-2 Monolayers Mimics Particle Uptake

Peter Pietzonka,[1,2] Barbara Rothen-Rutishauser,[1] Peter Langguth,[3] Heidi Wunderli-Allenspach,[1] Elke Walter,[1,4] and Hans P. Merkle[1]

Received January 21, 2002; accepted February 14, 2002

Purpose. The objective of this study was to evaluate nanoparticle uptake by the Caco-2 monolayer model *in vitro*. Special emphasis was placed on the localization and the quantification of the uptake of fluorescently labeled polystyrene and poly(lactic-co-glycolic acid) (PLGA) nanoparticles.

Methods. Intracellular fluorescence was localized by fluorescence and confocal laser scanning microscopy. Particle uptake was quantified either directly, by counting internalized nanoparticles after separation from the Caco-2 monolayers, or indirectly, by extraction of the lipophilic fluorescence marker. *In vitro* release studies of lipophilic markers from nanoparticles were performed in standard buffer systems and buffer systems supplemented with liposomes.

Results. Instead of uptake of polystyrene and PLGA nanoparticles by Caco-2 monolayers an efficient transfer of lipophilic fluorescence markers from nanoparticles into Caco-2 cells with subsequent staining of intracellular lipophilic compartments was observed. Whereas in standard buffer no release of fluorescent marker from polystyrene and PLGA nanoparticles was observed, the release studies using liposome dispersions as receiver revealed an efficient transfer of fluorescent marker into the liposome dispersion.

Conclusions. The results suggest that the deceptive particle uptake is caused by a collision-induced process facilitating the transfer of lipophilic fluorescent marker by formation of a complex between the nanoparticles and the biomembranes. Diffusion of the marker within this complex into lipophilic compartments of the cell strongly affects quantitative evaluation of particle uptake.

KEY WORDS: nanoparticle; Caco-2 cells; particle uptake; fluorescence; drug release.

INTRODUCTION

Several handicaps and barriers limit the oral bioavailability of drugs. Most relevant is the enzymatic metabolic barrier resulting in modification or cleavage of orally administered drugs and the physical barrier of the intestinal mucosa which relates to the low permeability of the tight junctional complexes in this epithelium. At the beginning of the last century it was generally understood that drugs only passed the intestinal epithelium when they were in a dissolved state. However, in 1906 Hirsch observed that in fact starch particles fed to rats were also absorbed and, therefore, found in the intestinal mucosa (1). Since the late nineteen fifties several authors investigated various particulate polymeric carriers and came up with the view that the particulate material itself, its particle size and the encapsulated drug exert major effects on the rate and extent of particulate uptake (2–6). The phenomena of uptake and transport through the epithelium of the intestinal tract are of the highest interest for the delivery of peptides, proteins and vaccines. Beneficial usage of this process could include the enhancement of drug absorption and bioavailability; the targeting of therapeutic agents to particular intestinal organs such as the gut associated lymphoid tissue (GALT) or the development of antigen carriers to achieve improved antigen presentation and mucosal immunity.

However, this field has not been without controversial discussions about the involved mechanisms and the extent of particle uptake by the intestine. Whereas Eldridge *et al.* (7) demonstrated that particle uptake was mainly through the Peyer's patches, other authors observed the transmucosal passage of particles to occur in the villous tissues adjacent to Peyer's patches or along the entire small intestine (8,9). The physical properties of the particles such as size, surface charge and hydrophobocity seemed to strongly influence their intestinal uptake. Several authors have extensively reviewed this subject (10–12).

The human colon adenocarcinoma cell line Caco-2 is a well-established cell culture model to study the intestinal permeability of drugs (13). Confluent Caco-2 monolayers form tight junctional complexes, exhibit dome formation and electrical properties similar to those of the intestinal epithelium. Previously several groups suggested the Caco-2 monolayers to function as a suitable *in vitro* model to investigate particle uptake into human intestine (12,14–16). Typically biodegradable nano- or microparticles made of poly(lactic acid) (PLA), or poly(lactic-co-glycolic acid) (PLGA) or non-biodegradable poly(styrene) (PS) particles were used for this purpose. Particles were labeled by loading them with fluorescent marker molecules like rhodamine B, fluorescein or coumarin-6 to provide both visual and quantitative evidence for cellular uptake and to avoid the problems associated with the use of radioactive materials.

However, fluorescence markers have been shown to cause experimental problems. For instance, Suh *et al.* (17) observed that marker molecules loaded into the matrix of particles or adsorbed to the particle surface during the preparation process might leak or dissociate from the particle. This may compromise the interpretation of particulate uptake data.

The objective of this study was to evaluate nanoparticle uptake by Caco-2 monolayers and their cellular localization. Biodegradable PLGA nanoparticles loaded with fluorescent markers and commercially available non-biodegradable polystyrene nanoparticles were used. Intracellular fluorescence was localized by fluorescence microscopy and confocal laser scanning microscopy (CLSM). Particle uptake was analyzed

[1] Institute of Pharmaceutical Sciences, ETH Zurich, Winterthurerstrasse 190, CH-8057 Zurich.
[2] Current address: Novartis Pharm Ag, Technical Research & Development, CH-4002 Basel.
[3] Institute of Pharmaceutical Technology and Biopharmacy, Johannes-Gutenberg-University, Staudinger Weg 5, D-55099 Mainz.
[4] To whom correspondence should be addressed. (e-mail: elke.walter@pharma.anbi.ethz.ch)

ABBREVIATIONS: CLSM, confocal laser scanning mircoscopy; GALT, gut associated lymphoid tissue; PBS, phosphate buffered saline; PLA, poly(lactic acid); PLGA, poly(lactic-co-glycolic acid); PS, poly(styrene).

0724-8741/02/0500-0595/0 © 2002 Plenum Publishing Corporation

by the quantification of extracted nanoparticles and by extraction of the fluorescence marker from the particles. Experiments were performed using viable and non-viable cell monolayers. Special attention was given to the effect of potential marker release from the nanoparticles. *In vitro* release studies in the presence of liposomes were used as a tool to evaluate the transfer of highly hydrophobic markers upon physical contacts between nanoparticles and the lipid bilayers. In this context we will evaluate the potential of collision-induced transfer of lipophilic markers from the nanoparticles into into Caco-2 monolayers as a mechanism to mimic the uptake of particulate matter.

MATERIALS AND METHODS

Chemicals

Polystyrene nanoparticle suspension (Fluoresbrite Plain YG, mean diameter 0.5 μm, particle concentration 2.69%, w/w) was purchased from Polysciences Inc. (Warrington PA, USA), poly-(DL-lactic-co-glycolic acid) (Resomer 752) was obtained from Boehringer-Ingelheim (Ingelheim, Germany). Nile red was from Aldrich Chemie (Buchs, Switzerland), coumarin 6 was from Acros Organics (Geel, Belgium). Polyvinyl alcohol 15'000 from Fluka Chemie AG (Buchs, Switzerland) was used as emulsion stabilizer. Oregon green phalloidin, rhodamin phalloidin and Hoechst 33342 were from Molecular Probes (Leiden, Netherlands). Epikuron 145 V was a gift from Lucas Meyer GmbH (Hamburg, Germany). All other chemicals were supplied by Fluka (Buchs, Switzerland) and were of chemical grade. If not otherwise specified cell culture media were supplied from Gibco, Life Technologies AG (Basel, Switzerland).

PLGA Nanoparticle Preparation

PLGA nanoparticles were prepared by using a modified oil-in-water solvent evaporation method according to (18). Briefly, 500 mg PLGA was dissolved in 10 ml methylene chloride, and 0.1% nile red or coumarin 6 were added. The solution was poured into 50 ml cold water containing 0.2% PVA as emulsifier. The emulsion was homogenized on ice for 5 min by ultrasonication (Vibra Cell, Sonics & Materials, Newtown Connecticut) and transferred into a reaction vessel. The solvent was evaporated using reduced pressure under constant stirring. After 3 h the nanoparticles were purified using gel filtration as described by Beck *et al.* (19). The gel filtration medium was Sephadex G 50 medium (Amersham Pharmacia Biotech, Uppsala, Sweden). The nanoparticles were freeze dried after separation of free marker and stored at 4°C.

Nanoparticle Characterization

Particle diameters were analyzed by field emission scanning electron microscopy (Hitachi S-700, Tokyo, Japan) after drying in a critical point dryer using CO_2 as the transitional solvent and by photon correlation spectroscopy (Nicomp 370, Particle Sizing Systems, Santa Barbara California). Nanoparticles were visualized by fluorescence microscopy (Axiovert 35, Zeiss AG, Zurich, Switzerland).

Cell Culture

Caco-2 cells (passage 72 and 76) were a gift from the Institute of Physiology of the University of Zurich, Switzerland. They were seeded at a density of 25,000 cells/cm^2 on glass cover slides or in tissue culture treated 6-wells (diameter 3.6 cm, Techno Plastic-Products AG, Trasadingen, Switzerland) and grown in an atmosphere of 5% CO_2, using Dulbecco's modified Eagle's Medium with Glutamax-I, sodium pyruvate and 4.5 g/L glucose. The medium was supplemented with 16.5% fetal calf serum and 0.1 mM nonessential amino acids. Cells were grown for 14 to 16 days and medium was changed every other day.

Particle Uptake Studies

Polystyrene and PLGA nanoparticles were suspended in transport buffer (TB) containing 1 mM $CaCl_2$, 3 mM KCl, 1 mM $MgCl_2$, 135 mM NaCl, 1 mM NaH_2PO_4 and 5 mM D-glucose at a concentration of 100 μg/ml for polystyrene and 10 mg/ml for PLGA nanoparticles. The pH was adjusted to 6.8 with 25 mM HEPES. Prior to selected experiments cells were fixed with ice cold 3% paraformaldehyde in phosphate buffered saline (PBS; 2.7 mM KCl, 1.5 mM KH_2PO_4, 135 mM NaCl and 8 mM Na_2HPO_4 adjusted to pH 7.4) for 30 m. Nanoparticle suspensions were prewarmed to 37°C and added to the cell monolayer. Monolayers were incubated for 60 min and washed twice with TB and three times with PBS.

The viability of the cell monolayers was checked using a live/dead kit (Molecular Probes, Leiden, The Netherlands) after incubation for 30 min with a solution of 4 μM ethidium homodimer-1 and 2 μM calcein AM in PBS. Samples were cautiously rinsed with fresh PBS and analyzed by fluorescent microscopy.

Microscopy

Caco-2 monolayers were fixed and stained with Hoechst 33342 (nuclei) and rhodamine (red fluorescence) or oregon green (green fluorescence) phalloidin (F-actin) depending on the respective marker of the nanoparticles and mounted in Lisbeth's imbedding medium. The samples were analyzed with either light and fluorescent microscopy (Axiovert 35, Zeiss AG, Zurich, Switzerland) or confocal laser scanning microscopy (CLSM) (LSM 410, Zeiss AG, Zurich, Switzerland) equipped with an Ar UV excitation laser (excitation 363 nm), an Ar excitation laser (excitation 488 nm) and a HeNe excitation laser (excitation 543 nm) within 24 h. Images were processed on a Silicon Graphics workstation using IMARIS, a 3D multichannel image processing software for confocal microscopic images (Bitplane AG, Zurich, Switzerland).

Quantification of Nanoparticle Uptake

After particle incubation the Caco-2 monolayers were washed four times with TB and three times with PBS. Then 2 ml of distilled water were added to each well and the cells were homogenized within the well using ultrasonication (Vibra Cell, Sonics & Materials, Newtown Connecticut).

The number of particles taken up by Caco-2 monolayers after 30 m was determined by counting the fluorescent nanoparticles using a hemocytometer. Polystyrene and PLGA nanoparticle concentration in the incubation medium was de-

termined by the same method prior to the experiment. Results were expressed as percentage of number of particles found in the homogenate as compared to the total number of nanoparticles applied to the cells. For marker quantification the cell homogenate was freeze-dried. Methylene chloride was used to extract the marker from the freeze-dried residue. Quantification of the marker was performed by fluorimetry (Fluoromax, Spex Instruments, Middlesex, England). Control experiments confirmed a fluorescent marker recovery of over 95%.

Statistics

Each result is presented as mean ± SD with n = 3. Statistical significance was tested on the basis of Student's *t* test at 95% confidence intervals.

Release Studies

To study the transfer of fluorescence markers from nanoparticles to liposomes as a simplified lipid bilayer model, a liposomal dispersion was prepared by dissolving 0.5 mmol Epikuron 145V and 0.25 mmol cholesterol in a mixture of methylene chloride and methanol (2:1) in a round bottomed flask. The lipid film was dried in a rotary evaporator and hydrated with 43 ml TB for 30 min. Sonication on ice for 10 m resulted in liposomes with a mean diameter of 50–80 nm.

The *in vitro* release of fluorescence markers from PLGA nanoparticles and fluorescence labeled polystyrene nanoparticles in TB and in the liposomal dispersion was performed in two different experimental set-ups. Firstly, nanoparticles were dispersed in 2 ml prewarmed TB or in the liposomal dispersion and incubated at 37°C in rotating 4-ml-vials (Chromacol, London, UK) Samples were taken at regular time intervals and centrifuged. The supernatant was filtered through a 0.2 μm regenerated cellulose filter (Schleicher & Schuell, Dassel, Germany) to remove any residual particles, and freeze-dried. The resulting residue was extracted with methylene chloride and analyzed by fluorimetry as described above.

Secondly, to avoid direct contacts between the nanoparticles and the liposomes, an equilibrium dialysis set-up (Macro 2 equilibrium dialysis cells, Dianorm, Munich, Germany) was used with 2.0 ml nanoparticle dispersion in the donor and 2.0 ml liposomal dispersion in the receiver. A preconditioned dialysis membrane with a molecular weight cutoff of 10 kDa (Dianorm, Munich, Germany) separated the two chambers. The dialysis cells were slightly rotated at 37°C. Samples were taken at regular intervals and further processed as described above.

RESULTS

Electron microscopy of PLGA and polystyrene nanoparticles revealed their regular, spherical shape (Fig. 1). Generally, their surface morphology was smooth, without any visible pinholes or cracks. Although coumarin-6 labeled nanoparticles appear slightly smaller (Fig. 2 middle), the size distribution of all particles was unimodal with diameters in the total range of 300–600 nm and a mean diameter of 400–500 nm as confirmed by photon correlation spectroscopy. The encapsulation efficiency of nile red and coumarin-6 in PLGA nanoparticles after gel permeation chromatography was 70–80% of the theoretical content. The nominal load of the particles was 0.1 % (w/w).

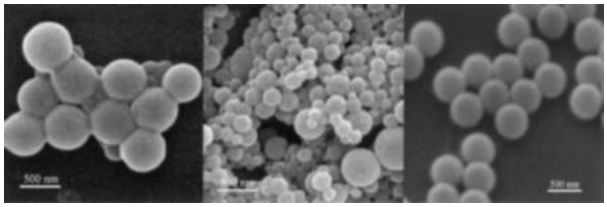

Fig. 1. SEM of nile red (left) and coumarin-6 (middle) labeled PLGA and labeled polystyrene nanoparticles (right panel). Spherical particles with a smooth surface and diameters in the total range of 300–600 nm and a mean diameter of 400–500 nm were obtained.

After 60 m incubation uptake of polystyrene nanoparticles into Caco-2 cells was very poor as shown by confocal laser scanning microscopy (CLSM). Typically, polystyrene particles were attached to the apical cell surface only (Fig. 2). No particles could be observed intracellularly or at the basolateral side. However, a highly fluorescent punctated pattern indicating spherical structures of up to 2 μm diameter was visible in the cells (Fig. 3), preferentially at the basolateral side. Note that nanoparticle diameters were generally smaller than 700 nm. Moreover, background fluorescence of the cells was significantly increased and, vs. controls without nanoparticles, intracellular structures became increasingly apparent (Fig. 4). Without nanoparticles background fluorescence was negligible. The observations were independent of particle type and fluorescence marker used. Similar results were already obtained after 30 min of incubation.

To rule out that the spherical structures represent nanoparticle agglomerates, nile red and coumarin-6 loaded PLGA nanoparticles were applied simultaneously. Fluorescence microscopy images using selective red respectively green filters demonstrated that red and green fluorescence were strictly colocalized (Fig. 5). An overlay of the images showed perfect congruence of the two patterns. This excludes that the observed fluorescent spheres represent single nanoparticles or nanoparticle agglomerates. Actual uptake of nanoparticles would have resulted in locally variable red and green staining instead of perfect uniformity of the pattern. As control the experiment was also performed with paraformaldehyde fixed, non-viable cells to exclude active uptake processes, e.g. by phagocytosis. As before green and red fluorescence was clearly colocalized, irrespective of the viability status of the samples.

Quantitative evaluation of particle uptake was performed by counting the number of nanoparticles extracted from cell monolayers. Within 30 m less than 1% of the totally administered polystyrene nanoparticles was adsorbed on the cells or found in the cells (Table I). When the nanoparticles were coated with human serum albumin or γ-globuline their interaction with the interface of the Caco-2 monolayer was significantly reduced. These findings were in strong contrast to the results obtained by analyzing the amount of fluorescence marker extracted from the cells. Up to 10% of the fluorescent markers from polystyrene nanoparticles were found in the cell monolayers (Fig. 6). Cell homogenates were found to be visually free of PLGA nanoparticles, but up to 7% of fluorescence marker were extracted from the cells.

The quantitative analysis of nanoparticle uptake into

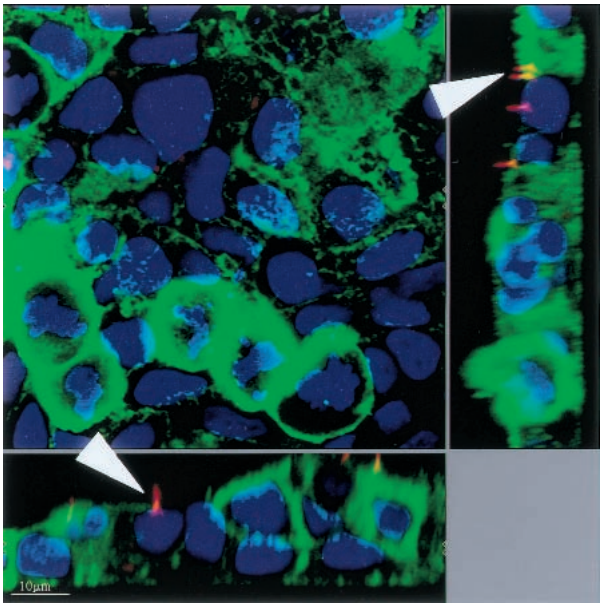

Fig. 2. CLSM of Caco-2 monolayer after incubation with polystyrene nanoparticles for 60 min (red). Typically, particles were only attached to the apical cell surface (arrowheads). Green: F-actin; blue: nuclei.

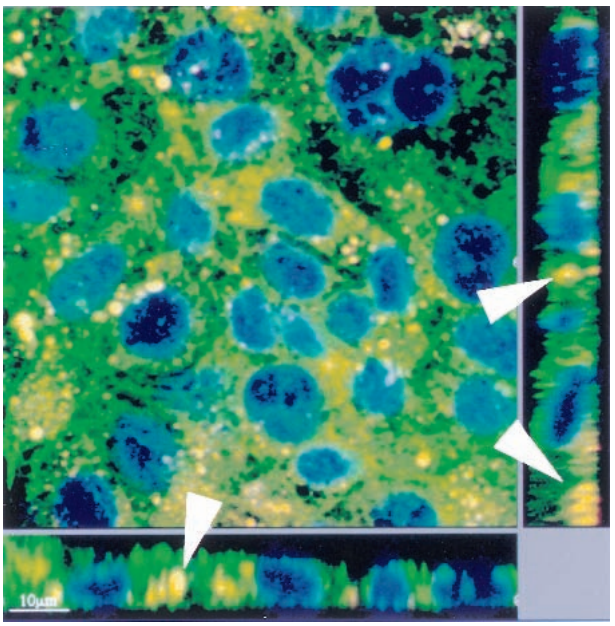

Fig. 3. CLSM image of Caco-2 cells incubated with PLGA nanoparticles for 60 min. Arrows indicate spherical structures (yellow) at the basolateral side of the cells. The size distribution of the structures indicates that they are bigger than the PLGA-nanoparticles (arrowheads). Green: F-actin; Blue: nuclei.

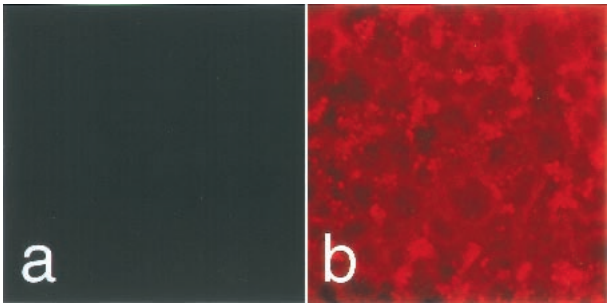

Fig. 4. Picture of Caco-2 cells before (a) and after (b) incubation with nile red loaded PLGA nanoparticles for 60 min. Spherical structures, probably intracellular lipid droplets, as well as the strongly increased background fluorescence are visible by fluorescence microscopy (Zeiss Axiovert 35).

Caco-2 cells was repeated with paraformaldehyde-fixed, non-viable cells. Interestingly, there was no significant difference between the uptake of marker into viable and non-viable cells independent of the carrier material and the type of fluorescence marker used (Fig. 6). These findings exclude relevant particle uptake by Caco-2 monolayers involving active mechanisms, e.g. by phagocytosis, which would be exclusive for viable cells. Instead of active nanoparticle uptake, we propose passive transfer of the marker partitioning of the hydrophobic markers from the nanoparticles into lipophilic cell compartments such as lipid membranes and vesicles.

To further confirm this mechanism we studied the *in vitro* release of the marker from PLGA and polystyrene nanoparticles into TB (Fig. 7). Overall marker release was low. After 3 h marker release from PLGA nanoparticles was slightly higher ~1%) than from polystyrene nanoparticles (<0.5%). This may be explained by traces of polyvinyl alcohol used as emulsion stabilizer during PLGA nanoparticle preparation.

The release studies of fluorescent nanoparticle dispersions in the donor chamber and liposome dispersion in the receiver chamber led to a linear release of the marker into the liposome compartment (Fig. 7). Polystyrene nanoparticles released about 1% marker after 60 m and 3.5% after 3 h, whereas PLGA particles released about 5% after 60 m and up to 50% after 3 h. Marker release was strongly enhanced when the nanoparticles were in direct contact with the liposome dispersion without the dialysis membrane in between. After 60 m about 5% of the marker from polystyrene particles and more than 50% of the PLGA markers were found to be transferred into the liposomes. After 60 m the release rates were approximately linear in both systems. No further release of markers was observed after 2 h.

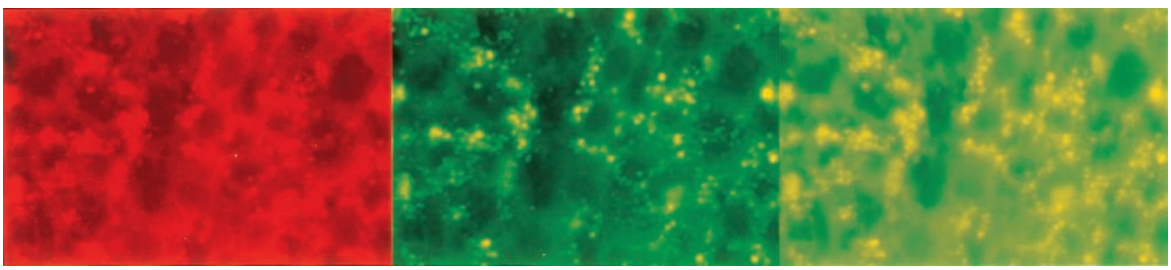

Fig. 5. Fluorescence microscopy of Caco-2 monolayers after simultaneous incubation with nile red and coumarin-6 labeled PLGA nanoparticles for 60 min. a red filter; b green filter; c overlay of a and b. Fluorescence in a and b is strictly colocalized.

Table I. Polystyrene (PS) Nanoparticles of Various Types Counted in Caco-2 Cells after 30 Minutes Incubation

Type of particle	Number of PS particles	Uptake* [%]
PS, uncoated	$2.29 \pm 0.33 \times 10^7$	0.8
PS, coated with human serum albumin	$5.83 \pm 0.26 \times 10^6$	0.2
PS, coated with γ-globuline	$5.90 \pm 0.16 \times 10^6$	0.2

* Numbers include both adsorbed and internalized particles.

DISCUSSION

In order to study particle uptake *in vivo* or *in vitro*, the use of fluorescently or radioactively labeled particles is the most common experimental approach found in the literature. We preferred fluorescent labeling because of easier handling. Thereby, particle uptake by cells becomes readily detectable by fluorescence microscopy or CLSM and the extent of particle uptake may be determined directly by flow cytometry or indirectly by quantitative extraction of the marker from the cells.

Because its structural and functional differentiation is similar to mature enterocytes, the Caco-2 monolayer model is an established *in vitro* tool to evaluate the intestinal permeability and metabolism of drugs (13). Reasonable correlations could be established between *in vivo* data and data obtained in Caco-2 monolayers (20). With respect to nanoparticles, Desai *et al.* demonstrated that uptake into Caco-2 cells was influenced by various parameters such as particle size and incubation time. An uptake efficiency of up to 41% was calculated after extracting the fluorescent marker from cell monolayers (14). In contrast, using CLSM, McClean *et al.* (16) reported that upon particle uptake in Caco-2 cells, the fraction of intracellularly detected particles was insignificant as compared to the number of particles totally administered. In the present study, using PLGA nanoparticles with loadings of highly hydrophobic fluorescent markers and commercially available polystyrene nanoparticles, we were unable to demonstrate significant particle uptake into or transport through Caco-2 cell monolayers by CLSM. According to our observations, the particles were only attached to the apical surface of the cells but not internalized. Successful internalization of particles was very rare. However, highly fluorescent, spherical structures in the cells raised questions about their nature and composition.

The contradictory findings in the quantitative uptake between the number of particles found in the cell homogenate and the amount of marker extracted from cells were obvious. The experimental results with a mixture of differently labeled PLGA nanoparticles applied on the Caco-2 monlayers indicate that the intracellular spherical structures were not single nanoparticles or nanoparticle aggregates. In addition, there was no visually detectable difference between Caco-2 monolayers incubated with fluorescent marker loaded particles or with an aqueous suspension of the pure marker alone (results not shown). Moreover, the equivalent amount of fluorescence marker extracted from both viable and non-viable (cross-linked with paraformaldehyde) monolayers led us to the conclusion that the transfer of hydrophobic fluorescent markers into Caco-2 cells occurred without the involvement of particle uptake.

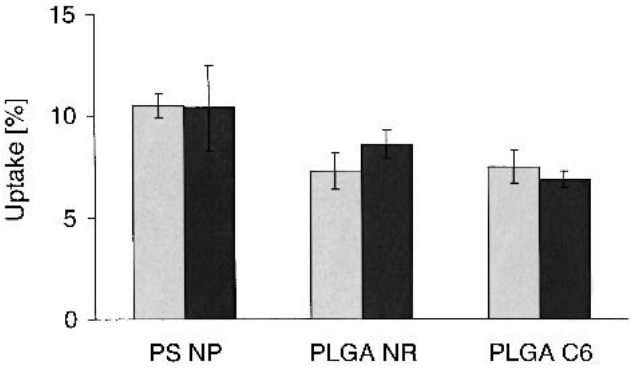

Fig. 6. Marker uptake from polystyrene (NP PS), nile red labeled PLGA (PLGA NR) and coumarin 6 labeled PLGA (PLGA C6) nanoparticles. No significant differences in marker uptake into viable (light grey) and non-viable (dark grey) Caco-2 monolayers were observed.

Greenspan *et al.* (21) reported nile red to be a powerful stain to visualize lipophilic cytoplasmatic components of fixed or viable macrophages and smooth muscle cells by fluorescence microscopy, e.g. intracellular lipid droplets. The authors concluded that highly lipophilic dyes could be used to

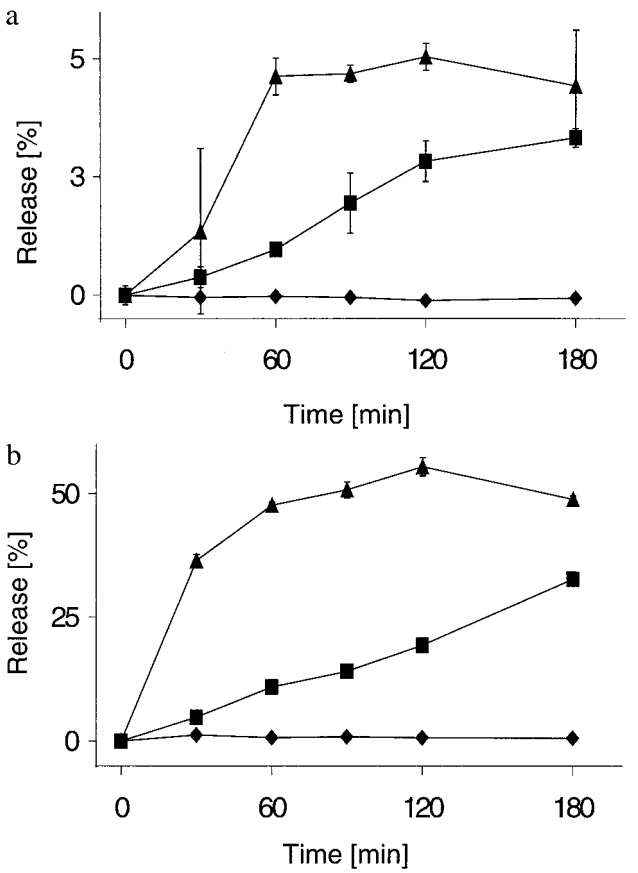

Fig. 7. Fluorescent marker release from polystyrene (Fig. 7a) and PLGA (Fig. 7b) nanoparticles into different receiver compartments: (♦) TB separated from the nanoparticle suspension by a dialysis membrane, (■) TB supplemented with liposomes separated from the nanoparticle suspension by a dialysis membrane, and (▲) TB supplemented with liposomes in direct contact (without a dialysis membrane) with the nanoparticle suspension.

stain cell membranes and intracellular lipophilic domains. According to Haynes and Cho (22) the transfer of lipophilic markers from particles into cells can occur through several processes: (i) exclusively by phagocytosis; (ii) by sequential dissociation of the marker from the particles, convective diffusion of the free marker into the medium and its subsequent partitioning into cells; and (iii) by a collision-induced non-phagocytic process entailing partitioning of a fraction of the entrapped substance directly from the surface of donor particles into the receiving cells.

Phagocytosis, an exclusive feature of viable cells, could be ruled out for our investigation. This was clearly demonstrated by equivalent intracellular staining patterns observed in both viable and non-viable cells. Therefore in accordance with our release studies we suggest that the diffusion process and the collision-induced process are responsible for the transfer of the marker into the cells. The possibility of direct contacts between the particles and the cell membrane seems to accelerate the transfer of the markers. Our release experiments demonstrated that in TB without liposomes only marginal marker release rates were detected. This was also expected from the low water solubility of the lipophilic markers. In the dialysis set-up with liposome dispersion in the receiver, marker release was increased. Linear release kinetics was observed. Only when the marker-loaded nanoparticles were in physical contact with the liposomal dispersion rapid transfer rates of the marker were observed. Therefore, we conclude from our results that direct transfer of the marker from the nanoparticles to the membrane leads to the staining of the cell wall and subsequently of the lipophilic domains of the cell. Previously, Mutsch *et al.* (23) postulated a lipid exchange mechanism involving collisional contacts to give rise to rapid exchange of lipids differing widely in chemical nature between liposomes and brush border vesicles. The exchange occurs by diffusion within the collisional complex formed between the liposome and brush border vesicles. Diffusion is considered to be a fast process (24) so that the collision rate is rate limiting rather than the diffusion of the molecules within the collision complex. Similarly, a collision model was postulated for a nile red oil-in-water emulsion (22). It was suggested that the transfer of nile red from various emulsions to macrophages may occurred via a collision-induced mechanism. By analogy we suggest that the transfer of lipophilic markers from nanoparticles into the liposomes is collision-induced and elicits substantial and immediate transfer of the lipophilic marker into the membrane, followed by a slower diffusion controlled process. We propose that the same mechanism applies for the uptake of lipophilic markers into Caco-2 monolayers, mimicking particulate matter uptake. Therefore, we suppose that active particle uptake by endocytosis by Caco-2 monolayers is probably the result of artefacts caused by the transfer of lipophilic markers from nanoparticles into lipophilic cell compartments. However, as a consequence, the same mechanism may offer new strategies for the efficient delivery of drugs with poor aqueous solubility and high lipophilicity to cells of the mammalian body.

Although we employed liposomes to clarify the mechanism of marker exchange on membrane interfaces, these experiments do not linearly compare with the quantitative marker uptake in cell monolayers. Liposomes represent a very simplified model for mimicking cells. Confluent cellular monolayers contain a larger variety of acceptor compartments, such as the cytosol, intracellular organelles and intercellular spaces that may also be of different volume as compared to liposomes. Thus, differences in hydrophilicity of the marker used in the PLGA particles and polystyrene particles may result in a different distribution behavior of cells vs. liposomes. In addition, the chemical nature of the fluorescent marker incorporated into the commercial polystyrene nanoparticles is not clear due to proprietary reasons. No information is available from the manufacturer whether the fluorescent label is covalently linked or just incorporated into the polystyrene nanoparticles. Anyway, our data strongly suggest that at least a significant portion of the label is not covalently bound to the polymer but sufficiently free to allow its immediate transfer to cells or lipid bilayer structures.

In summary, our study demonstrates that polystyrene and PLGA nanoparticles were not taken up by Caco-2 monolayers. Instead we observed an efficient transfer of lipophilic fluorescence markers from nanoparticles into Caco-2 cells with subsequent staining of intracellular lipophilic compartments and thereby mimicking particle uptake into the cell monolayers. Whereas *in vitro* release studies using standard PBS buffer systems showed no release of lipophilic fluorescent marker from polystyrene and PLGA nanoparticles, further *in-vitro* release studies using liposome dispersions as receiver revealed an efficient transfer of fluorescent marker into the liposome dispersion. The results suggest that the deceptive particle uptake is caused by a collision-induced process facilitating the transfer of lipophilic fluorescent marker by formation of a complex between the nanoparticles and the biomembranes of the Caco-2 cells or the liposomes, followed by a diffusion of the marker within this complex according to the concentration gradient. Consequently, the extent of transfer of lipophilic markers from nanoparticles is facilitated by a collision-induced process therefore affecting quantitative evaluation of particle uptake. In conclusion, our study questions previous nanoparticle uptake studies into Caco-2 cell monolayers and intestinal epithelium based on nanoparticles with non-covalently linked lipophilic markers.

ACKNOWLEDGMENTS

The authors acknowledge the following contributions: Ernst Wehrli for electron microscopy and Seraina Johner for her support in the cell culture experiments. This work was supported by the Stipendienfonds der Basler Chemischen Industrie.

REFERENCES

1. R. Hirsch. Das Vorkommen von Stärkekörnern im Blut und im Urin. *Z. Exp. Pathol. Ther.* **3**:390–392 (1906).
2. J. M. Payne, B. F. Sansom, R. J. Garner, A. R. Thompson, and B. J. Miles. Uptake of small particles (1-5 um) by the alimentary canal of the calf. *Nature* **188**:586–587 (1960).
3. E. Sanders and C. Ashworth. A study of particulate intestinal adsorption and hepatocellular uptake. Use of polystyrene latex particles. *Exp. Cell Res.* **22**:137–145 (1961).
4. M. E. LeFevre and D. D. Joel. Intestinal absorption of particulate matter. *Life Sci.* **21**:1403–1408 (1977).
5. M. E. LeFevre, J. W. Vanderhoff, J. A. Laissue, and D. D. Joel. Accumulation of 2-micron latex particles in mouse Peyer's patches during chronic latex feeding. *Experientia* **34**:120–122 (1978).
6. B. Muller and J. Kreuter. Enhanced transport of nanoparticle

associated drugs through natural and artificial membranes—a general phenomenon? *Int. J. Pharm.* **178**:23–32 (1999).
7. J. H. Eldridge, C. J. Hammond, J. A. Meulbroek, J. K. Staas, R. M. Gilley, and T. R. Tice. Controlled vaccine release in the gut-associated lymphoid tissues. I: Orally administerd biodegradable microspheres target the Peyer's patches. *J. Control. Release* **11**: 205–214 (1990).
8. G. M. Hodges, E. A. Carr, R. A. Hazzard, C. O'Reilly, and K. E. Carr. A commentary on morphologic and quantitative aspects of microparticle translocation across the gastrointestinal mucosa. *J. Drug Targ.* **3**:57–60 (1995).
9. J. Limpanussorn, L. Simon, and A. D. Dayan. Transepithelial transport of large particles in rat: a new model for the quantitative study of particle uptake. *J. Pharm. Pharmacol.* **50**:753–760 (1998).
10. J. Kreuter. Peroral administration of nanoparticles. *Adv. Drug Deliv. Rev.* **7**:71–76 (1991).
11. A. T. Florence. The oral absorption of micro- and nanoparticulates: Neither exceptional nor unusual. *Pharm. Res.* **14**:259–266 (1997).
12. F. Delie. Evaluation of nano- and microparticle uptake by the gastrointestinal tract. *Adv. Drug Del. Rev.* **34**:221–233 (1998).
13. P. Artursson. Cell cultures as models for drug absorption across the intestinal mucosa. *Crit. Rev. Ther. Drug Carrier Syst.* **8**:305–330 (1991).
14. M. P. Desai, V. Labhasetwar, E. Walter, R. J. Levy, and G. L. Amidon. The mechanism of Uptake of biodegradable microparticles in Caco-2 cells is size dependent. *Pharm. Res.* **14**:1568–1573 (1997).
15. T. Jung, W. Kamm, A. Breitenbach, E. Kaiserling, J. X. Xiao, and T. Kissel. Biodegradable nanoparticles for oral delivery of peptides: is there a role for polymers to affect mucosal uptake? *Eur. J. Pharm. Biopharm.* **50**:147–160 (2000).
16. S. McClean, E. Prosser, E. Meehan, D. Omalley, N. Clarke, Z. Ramtoola, and D. Brayden. Binding and uptake of biodegradable poly-dl-lactide micro- and nanoparticles in intestinal epithelia. *Eur. J. Pharm. Sci.* **6**:153–163 (1998).
17. H. Suh, B. Jeong, F. Liu, and S. W. Kim. Cellular uptake study of biodegradable nanoparticles in vascular smooth muscle cells. *Pharm. Res.* **15**:1495–1498 (1998).
18. H. Jeffery, S. S. Davis, and D. T. O'Hagan. The preparation and characterisation of poly(lactide-co-glycolide) microparticles: I: Oil-in-water emulsion solvent evaporation. *Int. J. Pharm.* **77**:169–175 (1991).
19. P. Beck, D. Scherer, and J. Kreuter. Separation of drug-loaded nanoparticles from free drug by gel filtration. *J. Microencaps.* **7**:491–496 (1990).
20. S. Yee. In vitro permeability across Caco-2 cells (colonic) can predict in vivo (small intestinal) absorption in man—Fact or myth. *Pharm. Res.* **14**:763–766 (1997).
21. P. Greenspan, E. P. Mayer, and S. D. Fowler. Nile Red: A selective fluorescent stain for intracellular lipid droplets. *J. Cell Biol.* **100**:965–973 (1985).
22. L. C. Haynes and M. J. Cho. Mechanism of Nile red transfer from o/w emulsions as carriers for passive drug targeting to peritoneal macrophages in vitro. *Int. J. Pharm.* **45**:169–177 (1988).
23. B. Mutsch, N. Gains, and H. Hauser. Interaction of intestinal brush border membrane vesicles with small unilamellar phospholipid vesicles. Exchange of lipids between membranes is mediated by collisional contact. *Biochem.* **25**:2134–2140 (1986).
24. H. Trauble and E. Sackmann. Studies of the crystalline-liquid crystalline phase transition of lipid model membranes. 3. Structure of a steroid-lecithin system below and above the lipid-phase transition. *J. Am. Chem. Soc.* **94**:4499–4510 (1972).